Published in final edited form as:
Biomaterials. 2010 May ; 31(14): 4064–4072. doi:10.1016/j.biomaterials.2010.01.101.

The ability of corneal epithelial cells to recognize high aspect ratio nanostructures

Elizabeth J. Tocce[1], **Valery K. Smirnov**[2], **Dmitry S. Kibalov**[2], **Sara J. Liliensiek**[1], **Christopher J. Murphy**[3,*], and **Paul F. Nealey**[1,*]

[1]Chemical & Biological Engineering, University of Wisconsin, Madison

[2]Wostec, Inc., Moscow, Russia

[3]Schools of Medicine and Veterinary Medicine, University of California, Davis

Abstract

The basement membrane of the human corneal epithelium comprises topographic features including fibers, pores, and elevations with feature dimensions on the order of 20-400 nm. Understanding the impact of sub-micron and nanotopography on corneal cell behavior will contribute to our understanding of biomechanical cues and will assist in the design of improved synthetic corneal implants. We utilized well defined ridge and groove wave-like nanostructures (wave ordered structures, WOS) of 60-140 pitches (30-70 nm ridge widths) and 200 nm depths to assess human corneal epithelial cell (HCEC) contact guidance and to establish HCEC contact acuity defined as the lower limit in feature dimensions at which cells respond to biomimetic topographic cues. Results using the WOS substrates demonstrate that HCEC contact acuity is in the range of 60 nm pitch for cells in a serum-free basal medium (EpiLife®) and in the range of 90 nm pitch for cells in epithelial medium. To further investigate the influence of HCEC contact acuity in the presence of larger topographic cues, we fabricated 70 nm pitch WOS overlaid parallel to the top of the ridges of 800-4000 nm pitch. HCEC cultured in epithelial medium demonstrate a significant increase in the percent of cells aligning to 4000 nm pitch topography with WOS overlay compared to controls (both flat and 70 nm WOS alone) and 4000 nm pitch topography alone. These results highlight the significance of the lower range of basement membrane scale topographic cues on cell response and allow for improved prosthetic design.

Introduction

To develop improved corneal prosthetics, it is important to understand how biologically relevant biophysical cues impact cellular behavior. This approach in the design of biomaterials for tissue regeneration aims to fabricate scaffolds that mimic the natural *in vivo* extracellular environment. *In vivo*, the basal layer of human corneal epithelial cells (HCEC) adheres to the underlying corneal stroma through the basement membrane (BM). Through its intrinsic biochemical constituents and biomechanical attributes, the BM provides both chemical and

*Corresponding Authors: Christopher J. Murphy, Department of Ophthalmology and Vision Science, School of Medicine, Department of Surgical and Radiological Sciences, School of Veterinary Medicine, University of California, Davis, Phone: (530) 754-0216, Fax: (530) 752-6161, murphy@corl.vetmed.wisc.edu, cjmurphy@ucdavis.edu, Paul F. Nealey, Department of Chemical and Biological Engineering, University of Wisconsin, Madison, Madison, WI 53706, Phone: (608) 265-8171, Fax: (608) 265-3557, nealey@engr.wisc.edu.

mechanical cues that impact cell behavior [1]. Researchers have characterized biophysical properties of the native BM from several different epithelial tissues across a range of species and have found that the BM is a flexible, protein-based substrate comprising nano to submicron scale topographical features [2-13].

Chemical composition, substrate modulus and topographic features characteristic of those of the BM can be manipulated to control cellular response *in vitro* and can be exploited in the design of prosthetics. For example, BM components have been show to enhance keratinocyte attachment [14], and impact the development of functional mammary epithelial tissue [15, 16]. Studies have also shown that simply changing the modulus of the substrate can affect cell morphology [17,18], motility [19,20], and even induce stem cells to differentiate down specific lineages [21,22]. These reports have all made major strides towards understanding and controlling the biophysical cues to elicit specific cell response.

Recent research from our group and others has focused on understanding cell response to topographical cues with dimensions from nano (1-100 nm) to sub-micron (100-1000 nm) to micron-scale (>1000 nm). The effects of micron-scale topography on cell function and phenotype has been widely characterized for multiple cell types (see reviews [23-25]). Although interesting, studies using micron-scale topography do not investigate the effects of biologically relevant length scales (approximately 20-400 nm for the corneal BM, [6]). To bridge the gap between research that focused mainly on micron-scale topographical cues and the upper range of dimensions found in the BM (100-400 nm), we have studied the impact of sub-micron and micron-scale features on HCEC behavior. We have demonstrated that a menu of fundamental cellular behaviors, including alignment [26-29], proliferation [30], adhesion [31,32], migration [26], morphology [26], and differentiation [33] all elicit different cell phenotypes in the upper range of dimensions found in the BM (200-800 nm) compared to micron scale dimensions. For example, cells on sub-micron topography with geometries of both ridges/grooves and holes have been shown to more strongly adhere to the substrate compared to micron scale and flat controls [31,32]. This transition in cell response to topographic cues correlates to the largest feature dimensions characteristic of the native corneal epithelium BM (several hundreds of nanometers [6]).

To probe the effects of topographic features that are in the lower range of feature dimensions observed in the native BM, different methods have been utilized to fabricate lateral features in the range of 20-100 nm, including nanotubes [34], electrospun fibers [35], and lithographically defined holes [36] and ridges [37]. Many of these studies utilize topography with minimal depth (less than 80 nm), which may limit cellular response to the lateral dimension. Recent studies have shown that depth of the features can dictate the extent to which the cells will respond to a given lateral dimension. We have previously demonstrated that on pitches ranging from 400 nm to 4000 nm, primary HCEC do not preferentially align to the underlying topography when the depth is less than 150 nm [38]. However, HCEC elongation and alignment response is enhanced by increasing the depth of the grooves from 150 nm to 800 nm [26,38]. To understand the influence of biologically relevant topographic features, we must investigate the impact of features with dimensions that compare to the smallest BM dimension and have appreciable depth to elicit cellular response.

The aim of the research presented here is to determine the lower limit in substratum feature dimensions to which HCECs will exhibit contact guidance. We have used the term “contact acuity” due to the parallels with visual acuity, that is, the ability to resolve two points in space as separate. These experiments require the development of well defined nano-scale structured surfaces having features with pitches of 60-140 nm (widths of 30 to 70 nm). For cell culture studies, the requirement for producing large numbers of substrates with relatively large patterned areas limits the fabrication methods that can be used. For example, current

lithographic processes, like electron beam lithography (EBL), can be used to fabricate nanometer scale lateral dimensions, but are cumbersome when attempting to pattern areas on the order of square millimeters. Additionally, it is time consuming and expensive to produce substrates using EBL.

To circumvent these issues, we obtained nanostructured surfaces from Wostec, Inc., Moscow, Russia. Surfaces were produced using a low-energy ion bombardment process that creates wave ordered structures (WOS) with pitches that are dependant on the ion bombardment conditions [39]. The process quickly produces large patterned areas on the order of 10 mm^2. The WOS fabrication also meets previously described criteria including good control over lateral dimension and appreciable feature depth. Resulting WOS substrates with pitches of 60, 90, and 140 nm, and depths of 200 nm were used to assess HCEC contact acuity in two different cell culture mediums: epithelial medium and EpiLife® medium.

Materials and Methods

Fabrication of 60, 90, 140 nm WOS substrates

To determine the contact acuity of primary human corneal epithelial cells (HCEC) we fabricated substrates with wave-like ridge and groove features, referred to as wave ordered structures (WOS). Substrates were prepared using a proprietary lithography-free nanofabrication technology developed by Wostec, Inc (Moscow, Russia). The technology is based on a self-forming ion beam process resulting in quasiperiodic WOS as wave-like nanopatterns on the silicon surfaces. First, WOS formation is induced by oblique flow of low energy 1-8 keV nitrogen ions [39]. The resulting quasiperiodic structures are subsequently used as a hard nanomask on silicon chips. In this work, WOS-nanomasks with average pitches of 60, 90, and 140 nm (approximately 30, 45, and 70 nm ridge widths, respectively) were formed. Then silicon chips were reactive ion etched (RIE) in a RIE tool using Cl_2 based plasma providing highly selective etching of silicon with respect to silicon nitride of WOS-nanomask [40]. For each WOS pitch the RIE process was adjusted to an etch depth of about 200 nm.

Fabrication of WOS overlay onto ridge-groove features

To test the combinatorial effects of sub-acuity WOS topography and larger sub-micron and micron-scale topography, WOS topography was overlaid parallel to topographic features on silicon chips containing 6 regions of groove and ridge patterns. First, we fabricated the larger silicon features with a depth of 300 nm and pitches of 4000 nm, 2000 nm, 1600 nm, 1200 nm, 800 nm, and 400 nm and flat controls as outlined in our previous work [26,27]. Briefly, a silicon wafer was coated with UV3 photoresist (Shipley, MA) and exposed to x-rays through a mask containing the desired topographic pattern. The exposed wafer was developed (MF320, Shipley, MA) and subsequently reactive ion etched (RIE) using a Trion Phantom I etcher with a SF_6 and C_4F_8 plasma. The wafer was cleaned using piranha solution of 3:7 parts hydrogen peroxide (30% in water, Fischer Scientific, NJ) to sulfuric acid (Fischer Scientific, NJ) for 30 minutes and then diced into small chips using a silicon dicing saw such that each chip contained all six pitches and flat control. Next, we overlaid 70 nm WOS features on some of the chips using the protocol described in the previous section. WOS-nanomasks with an average pitch of 70 nm were fabricated on our existing silicon chip patterns by directing an oblique nitrogen ion beam resulting in WOS features aligned parallel to the lithographically defined grooves and ridges. Oblique ion bombardment resulted in partial coverage of the groove bottoms by the WOS-nanomask due to shadowing of the ion flow by the groove sidewalls. The tops of lithographically defined ridges were entirely covered by the WOS-nanomask. Silicon chips were etched to a depth of about 200 nm in a RIE tool using Cl_2 based plasma.

SEM confirmation of topography

Prior to plating cells for each experiment on topographically patterned silicon substrates, the silicon substrates were cleaned by immersing them in a piranha solution for 30 minutes. The solution contained 3:7 parts hydrogen peroxide (30% in water, Fischer Scientific, NJ) to sulfuric acid (Fischer Scientific, NJ). Substrates were then rinsed twice in Milli-Q-H_2O (Millipore, MA) and dried under a flow of nitrogen. The fidelity of the substrate topography was confirmed using a LEO-1550 VP field-emission scanning electron microscope (SEM, magnification of 20 KX, accelerating voltage of 10 kV). Substrates containing major defects were eliminated from the study. Substrates were cleaned and used up to 5 times.

Preparation of substrates for cell culture

In preparation for cell seeding, one silicon chip was placed into a single well of a 12-well tissue culture plate (BD Falcon, CA). All substrates were soaked in 70% ethanol for 10 minutes, rinsed 3 times with sterile 1× phosphate buffered saline (PBS, pH 7.2, Invitrogen, CA), air dried and exposed to UV light for 30 minutes in a sterile laminar flow hood.

Primary human corneal epithelial cell harvest and culture

Human cadaver corneas were graciously donated by the Lions Eye Bank of Wisconsin, Madison or the Missouri Lions Eye Bank (Columbia, MO). The primary human corneal epithelial cells (HCEC) were harvested as described in [26]. Following disaggregation of HCEC with dispase solution (1.2 units/ml at 37° C for 4 hours, Boehringer Mannheim, Germany) cells from 2-4 corneas were centrifuged and resuspended in either epithelial medium or in EpiLife® medium without calcium and phenol red (Invitrogen, CA). Epithelial medium contained a 3:2 ratio of Ham's F12:Dulbelco's Modified Eagles medium (DMEM) (Invitrogen, CA), supplemented with 2.5 % (v/v) fetal bovine serum (FBS), 0.4 μg/ml hydrocortisone, 8.4 ng/ml cholera toxin, 5 μg/nl insulin, 24 μg/ml adenine, 10 ng/ml epidermal growth factor, 100 units penicillin, and 100 μg/ml streptomycin [41,42]. HCECs in epithelial medium were plated into 100 mm tissue culture plates containing a mitomycin-c treated Swiss 3T3 fibroblast layer. EpiLife® medium was supplemented with a proprietary combination of bovine serum albumin, bovine transferrin, hydrocortisone, recombinant human insulinlike growth factor type-1, prostaglandin, and recombinant human epidermal growth factor (Human Corneal Growth Supplement, Invitrogen, CA). Cells in EpiLife® medium were plated into 100 mm tissue culture plates coated with fibronectin and collagen (FNC coating mix, AthenaES, MD). All HCECs were incubated at 37°C and 5% CO_2 until they reached approximately 70% confluence. Cells were used between passages 1 and 2. For all experiments, 5 replicates of each substrate were used and the cells were plated at a density of 10,000 cells per cm^2. All cells were incubated for 12 hours after plating to allow for attachment and spreading.

Immunocytochemistry

To investigate HCEC elongation and alignment response to topographically patterned substrates, we stained for actin-filaments (cell shape) and nuclei (cell number). Following 12 hours of incubation, the surfaces were rinsed with 1× PBS. The surfaces were then fixed with 4% paraformaldehyde-PBS (Electron Microscopy Sciences, PA) at room temperature for 20 minutes. Following a 1× PBS wash, the cells were permeabilized with 0.1% (v/v) triton X – 100 (Sigma-Aldrich, MO) in 1× PBS for 7 minutes, washed in 1× PBS for 10 minutes, and then immersed in 1% (w/w) bovine serum albumin (Sigma-Aldrich, MO) in 1× PBS for 20 minutes to block non-specific binding. Cells were rinsed with 1× PBS for 10 minutes, then incubated with 5 μg/ml of TRITC-phalloidin (Sigma-Aldrich, MO) containing 0.1 μg/ml 4′,6-Diamidino-2-phenylindole (DAPI) (Invitrogen, CA) in 1× PBS for 40 minutes, to label both filamentous actin (red), and the nucleus (blue). Following a final rinse with 1× PBS, each

substrate was mounted between a glass slide and a glass coverslip using DABCO® (Fluka, Switzerland), an anti-fading mounting medium, and sealed with clear nail polish.

Quantification of cell shape and orientation

Samples were imaged using a Zeiss Axiovert 200M fluorescent microscope (Zeiss, Germany). Images of fluorescent cells on each of the chips were obtained using a 10× objective lens. For substrates containing only WOS (60, 90, and 140 nm), at least 8 images were taken for each pitch, flat and tissue culture polystyrene (TCPS) controls. For topographic substrates containing 6 ridge/groove widths, at least four images were taken of each pattern pitch and flat areas on the same sample. On average, 10-15 single cells per image were present per pattern size thus allowing approximately 80-120 cells on WOS only substrates and 40-60 cells on the larger 6 ridge/groove pitch topographies to be analyzed per pattern. Image analysis was performed using AxioVision software (Zeiss, Germany). The cell angle of alignment and cell elongation factor measurements were collected from the images and sorted using parameters previously described by our group [26,29]. In brief, to obtain single cell analysis, all cells in contact with other cells and cells in contact with the edge of the image were manually removed from the data sets. Elongation was quantified by an extension factor, characterized as the ratio between the length, *l*, of the longest axis of the cell and the length, *w*, of the longest axis perpendicular to *l* [27]. A cell was deemed elongated if the extension factor (*l*/*w*) was greater than 1.3. Only cells that were elongated were considered aligned at their angle of alignment. Alignment angle was defined as the angle between the long axis of the cell and the long axis of the underlying topographic pattern. A cell was considered aligned parallel if the angle was less than 10° and perpendicular if the angle was between 80° and 90°. For more detailed analysis, cells were sorted into 10 degree increments (0-10, 10-20, 20-30, 30-40, 40-50, 50-60, 60-70, 70-80, and 80-90 degrees). Results represented the arithmetic mean percent of the total single cell population. Each experiment contained 3-5 substrates per pitch.

Statistical analysis

Experiments were analyzed using analysis of variance (ANOVA). When variability was determined to be significant ($P < 0.05$), the Bonferroni multiple comparison test was used to determine significance ($P < 0.05$) between groups. Significance was further divided into "statistically significant" ($0.01 \leq P < 0.05$), "very significant" ($0.001 \leq P < 0.01$), and "extremely significant" ($P \leq 0.001$).

Results

SEM confirmation of substrate topography

Prior to using our silicon substrates for cell experiments, we measured the pitch, ridge width and depth of the WOS features. Scanning electron microscopy top-down images confirm that the lateral dimensions of the WOS were 60, 90, and 140 nm in pitch with approximately 1:1 ratio of ridge to groove width (Figure 1a). For each WOS substrate, the topographic pattern was continuous over an area of approximately 9-16 mm^2, with surrounding flat areas for control. The large patterned surface area per chip allows for significant number of cells (70-100 cells per surface) to be included in our studies. To verify and measure the depth, SEM cross-sectional images of 60, 90, and 140 nm WOS substrates were taken and confirmed that the depths were between 180 and 200 nm (Figure 1b).

Contact acuity in epithelial medium

The WOS topographically patterned substrates with pitches of 60, 90 and 140 nm were used to investigate the contact guidance for human corneal epithelial cells (HCECs) in epithelial medium. Twelve hours post plating, HCECs were fluorescently stained with TRITC-phalloidin

and DAPI, imaged and analyzed for cell elongation and alignment to the underlying topographic features (Figure 2).

Initially, we investigated the impact of WOS nanotopography cues on elongation of the HCE cells. Average elongation factors were about 1.6 for all WOS pitches and did not differ significantly from flat and TCPS controls. Next we quantified the percentage of cells aligned with the underlying topographic WOS features. We observed no significant alignment of cells in any one direction on flat silicon (Figure 3a) and TCPS controls (data not shown). Additionally, no contact guidance was observed on 60 nm pitch substrates (Figure 3b). Human CECs on the 90 nm WOS demonstrated a suggestive trend towards preferred parallel alignment (Figure 3c). On 90 nm WOS, the average percentage of cells with angles of alignment between 0 and 10 degrees was significantly more ($P < 0.05$) than all other angles (10-90 degrees) and about 5% above flat controls ($P<0.05$). We observed many cells elongating and aligning parallel on 140 nm pitch WOS (Figure 3d). Human CECs showed an extremely significant ($P<0.001$) increase of 15% in average parallel alignment on 140 nm pitch compared to the flat controls. With initiation of alignment at 90 nm pitch and strong parallel alignment at 140 nm the data suggest that contact acuity for HCEC in epithelial medium is around 90 nm pitch (45 nm ridges).

Contact acuity in EpiLife® medium

Soluble factors in cell culture conditions can significantly impact the cell response to external mechanical stimuli [22,26,33,43-45], thus we investigated how an alternative medium (EpiLife® medium compared to epithelial medium) would impact cell contact acuity. Human CECs in EpiLife® medium were stained, imaged and analyzed for elongation and alignment 12 hours after plating. On flat controls, HCECs averaged 8% alignment across all angles of alignment, and did not exhibit preferred orientation in any given direction. However, on all WOS substrates we observed perpendicular cell alignment trends. On 60 nm pitch WOS, statistically ($0.001<P<0.01$) more cells aligned perpendicularly (80-90 degrees) compared to all other angles (Figure 5b). Additionally, HCECs on 60 nm pitch WOS had about a 7% increase in perpendicular alignment compared to flat controls. Cells on 90 and 140 nm pitch WOS substrates also showed significantly ($P<0.001$) higher number of cells aligning perpendicularly than any other angle (Figures 5c and 5d), and had 20-40% increase in perpendicular alignment compared to flat ($P<0.001$ for both 90 and 140 nm). These data suggests that the contact acuity for HCEC in EpiLife® medium is below 60 nm pitch features (30 nm ridges).

Contact guidance on ridge-groove features with WOS overlay

We did not observe contact guidance of HCEC in epithelial medium on sub-90 nm WOS topography. However, we investigated whether or not sub-acuity scale WOS topographic features could modulate contact guidance when used in combination with larger scale topographic features. Seventy nanometer WOS was overlaid onto substrates with 5 distinct ridge-groove pitches of 800, 1200, 1600, 2000, and 4000 nm in silicon. The WOS topography was oriented parallel to the major axis of the underlying ridge-groove pattern.

We again used SEM to confirm the lateral and vertical dimensions. The depths of the larger ridge/groove features were approximately 400 nm while the depths of the overlaid 70 nm WOS were approximately 200 nm. Images also confirmed parallel arrangement of the WOS on the ridges of the 800-4000 nm pitches (Figure 6a). We noted that the transfer of the 70 nm WOS topography onto the 200 nm ridges of the 400 nm pitch topography was not as successful as compared to 800-4000 nm pitches. Effectively, the WOS fabrication process created 200 nm pitch features out of the original 400 nm pitch ridge/groove topography. These surfaces were removed from the study.

Human CECs in epithelial medium were plated onto substrates and incubated for 12 hours. Next, the cells were fixed, stained, imaged and analyzed for elongation and alignment. First, we analyzed HCEC contact guidance to 60, 90, and 140 nm WOS and observed similar parallel alignment as reported above. Next, we analyzed HCEC contact guidance to the 5 different ridge-groove pitches without the WOS overlay (800-4000 nm). Cells on control flat surfaces did not show preferred orientation while cells on topographically patterned substrates demonstrated preferred parallel alignment to 4000 nm pitches, and perpendicular on 800, 1200, 1600 and 2000 nm pitches. We observed an increase in parallel alignment on 4000 nm of approximately 25% compared to flat controls ($P<0.001$). Similarly, we observed approximately 15-25% increase in perpendicular cell alignment on 800-2000 nm pitch features compared to flat controls (data not shown).

Next, we analyzed HCEC on 800-4000 nm pitch topography with a 70 nm WOS-overlay. Cells on flat controls and 70 nm WOS alone did not show preferred orientation to the underlying topography. In contrast, cells on 800-2000 nm pitch topography with 70 nm WOS-overlay showed preferred alignment either parallel or perpendicular for all experiments (data not shown). Variation between six repeat experiments (4-5 substrates per experiment) was observed in the relative percentage of parallel and perpendicular alignment of cells on WOS-overlaid 800-2000 nm pitch topography. Although the preferred cell orientation (either parallel or perpendicular) varied between each experiments, the sum of the parallel (0-10°) and perpendicular (80-90°) orientation was consistently between 30 and 50% of the cell population, in contrast to cells on 70 nm WOS and flat which both had combined parallel and perpendicular alignment of 10-20%. Alternatively, we always observed parallel alignment of HCECs on 4000 nm pitch with WOS-overlay (Figure 7). Approximately 40-50% of the cells aligned parallel to the 4000 nm pitch features with the WOS-overlay compared to only 5-10% of the cells on flat controls and 70 nm WOS alone ($P<0.001$). Moreover, the percentage of cells that aligned parallel to 4000 nm pitch topography was consistently higher for substrates with the 70 nm WOS-overlay than without the overlay. Within each experiment, approximately 15-25% more cells aligned parallel on 4000 nm pitch topography with the WOS-overlay compared to without the overlay. This was extremely significant ($P < 0.001$) for each experiment.

Discussion

Our fundamental understanding of how basement membrane topography impacts cell behavior demonstrates that topography may play an important role in controlling cell behavior and should be considered in the design of improved corneal prosthetics. We have previously demonstrated the impact of topographical features on HCEC behavior with dimensions similar to dimensions in the upper range of features found in the native basement membrane (100-400 nm). Our current study is unique in that it allowed for measurements of HCEC response to dimensions related to the smallest features previously quantified in the basement membrane including average fiber and pore diameters of 46 and 92 nm [6]. To assess cellular response to topographical features, many studies have utilized micro-grooved substrates to measure cell contact guidance. Contact guidance has been shown to be an influential factor in improving *in vitro* cell extracellular matrix (ECM) protein production and organization in various tissue types including stromal fibroblasts [46] and neural cells [47]. Cell production of these ECM proteins is important in wound healing applications. The ability of groove-ridge topographic features to modulate cell contact guidance has been shown to be dependant on the cell type [29,48], lateral dimensions of the features [26,37], feature depth [26,37,38], and soluble environment [26,28].

In light of these studies we arrived at several crucial constraints that dictated the design of the substrates used in our studies which include: (1) the patterned area must be large enough to obtain robust cell data; (2) the depth of features must be sufficient to elicit cell response to

lateral pitch; and (3) the lateral pitch must be controllable and well defined. The WOS process allowed us to successfully incorporate all three design parameters.

As endpoints for HCEC response to WOS-defined substrates, we quantified multiple cell morphological responses, including cell area, elongation factor, and orientation to the underlying topography. Within each experiment, the total percent of cells elongated were independent of the pitch. In addition, there was no significant difference in HCEC area and elongation factor as a function of either size of topographic features or alignment angle. However, we observed that the scale of the features and the soluble environment significantly impacted HCEC contact guidance to the underlying topography.

To probe cell contact guidance of HCEC, we used WOS-defined substrates with feature dimensions of 60-140 nm pitch (30-70 nm ridge widths) and depths of 180-200 nm. Our observations indicate that there is a minimum length scale to which cells will respond through orientation to the topographic cues. This minimum length, or contact acuity, is in the range of native human corneal BM fiber dimensions (20-90 nm). Loesberg *et al.* [37] and Dalby *et al.* [36] also observed minimum lateral dimensions to which cells demonstrated interaction with topography. Loesberg *et al.* has shown that the smallest feature pitch to which rat dermal fibroblasts will align after 24 hours is 200 nm with 100 nm ridges and 77.4 nm depths [37]. Below 200 nm pitch, the fibroblast cells did not significantly align to the topography. Comparatively, Dalby *et al.* observed a decrease in cell area and an increase in the number of filopodia of immortalized human fibroblasts when seeded on pit-defined topography with 200 nm pitch (75 nm diameter pits and 100 nm depth). They also reported no significant differences in fibroblast cell area and number of filopodia between control smooth surfaces and 100 nm pitch pits (35 nm diameter pits and 50 nm depth) [36]. These studies suggest that cells exhibit contact guidance in response to substrate topographic features down to 200 nm in pitch. In contrast, we found HCECs respond to topographic features down to values of 60 nm pitch.

There are several possible explanations for our results demonstrating a lower acuity limit than previously reported studies. First, the depths of our WOS features were approximately four times greater than the depths utilized in the Loesberg and Dalby studies. Feature depth has been shown to directly impact cell response to lateral features, and we hypothesize that increasing the depth of the smaller features would elicit a greater degree of HCEC alignment. This is best supported by recent reports by Fraser *et al.* [38] and Biela *et al.* [48] that show no preferred cell alignment with shallow depths of 50-75 nm and 3-5 fold increase in parallel alignments with greater depths up to 200-880 nm. Another explanation for the differences between studies is that the minimum feature depth to elicit contact guidance is not absolute and appears to be cell type dependent. For example, Fraser *et al.* observed contact guidance of human stromal fibroblasts on topography with depths as low as 75 nm, while HCEC did not begin to align to the same topography until the depth was greater than 150 nm [38]. It would be interesting to investigate whether HCEC contact guidance to our smallest features is altered or enhanced with greater depth. We predict that there is a maximum depth, above which cell alignment plateaus, as seen with HCEC on features of 400-4000 nm pitch [38]. Knowing this maximum depth and the resulting cellular response would be an essential parameter in predicting and controlling response from cells when designing prosthetics.

In addition to heterogeneity in cell type specific response to depth, contact acuity could be inherently different for each individual cell type. Supporting this theory, we and others have observed that human fibroblasts in comparison to epithelial or endothelial cells, have a higher percent of alignment to grooved substrates [29,38,48]. As previously discussed, corneal fibroblasts will also respond to depths that are shallower than necessary to elicit response from corneal epithelial cells. Substrates utilized in our studies provide a means to investigate contact acuity differences between cell types.

Our studies have shown that cell contact acuity is influenced by nanotopography in conjunction with soluble factors. Our laboratory has previously shown that HCEC contact guidance, either parallel or perpendicular to the long axis of underlying features, is dependent on the soluble factors of the culture medium utilized. Human CECs in EpiLife® medium aligned perpendicular to 400 nm pitch (ridge and groove) features compared to parallel alignment when cultured in DMEM/F12 medium containing 10% FBS [28]. Similarly, we observed preferential perpendicular alignment of HCEC in EpiLife® medium and parallel alignment in epithelial medium 12 hours after plating on WOS surfaces. In addition to the differences in alignment, the ability of HCECs to respond to the features was also influenced by the soluble culture environment. Human CECs in epithelial medium demonstrated initiation of alignment to 90 nm pitch WOS. In contrast, HCEC in EpiLife® showed initiation of alignment at 60 nm pitch WOS. There are multiple different soluble or adsorbed chemical factors that could affect the intercellular mechanistic pathways leading to these different cell alignment responses. Rajnicek *et al.* [44] have reported that perpendicular alignment of embryonic rat hippocampal neurites on 1 μm wide features can be reduced by adding calcium channel blockers and high concentrations of protein kinase C inhibitors. However these inhibitors did not affect parallel hippocampal cell alignment to 4 μm wide features. These results suggest possible mechanistic pathways that control perpendicular alignment and that there may be different pathways that regulate parallel and perpendicular alignment.

In addition to understanding how topographical cues in lower range of dimensions found in the BM (20-100 nm) affects cell contact guidance, we also investigated whether nanoscale topography can modulate contact guidance when used in tandem with larger micron-scale topography. Seventy nm pitch WOS patterned surfaces alone failed to elicit contact guidance of HCECs in epithelial medium. However, we observed an increase in the percentage of cells aligned parallel to 4000 nm pitch with 70 nm WOS-overlay compared to 4000 nm pitch without WOS-overlay. This observation suggests that the smaller 70 nm topography has a subtle (and possibly an enhancing) effect on contact guidance. To our knowledge, there are limited reports that systematically incorporate two different topographic features onto one substrate for biological applications [49], and none that have utilized sub-acuity feature dimensions. We initially hypothesized that there may be a lower limit of lateral feature dimensions that could affect cellular contact guidance. However, our results suggest that even topographical cues that cannot elicit a macroscopic response from HCECs can still influence HCECs when used in combination with larger topography. Our results demonstrate that substrates with overlays of different feature length scales may be exploitable in the design of substrates to modulate cellular response to topographic cues. In addition, they provide a relevant basis to initiate further studies on the effects of hierarchal topographic cues on cell behaviors.

Conclusions

In order to investigate contact acuity and orientation of HCEC to topographic features with dimensions in the lower range of those observed in the native corneal basement membrane, we fabricated WOS substrates with ridges of 60-140 nm pitch (30-70 nm ridge widths) and depths of 200 nm. Our results indicate that HCEC contact acuity lies in the lower range of topographic feature dimensions found in the native corneal basement membrane and that contact acuity is dependant on the composition of the soluble culture environment. Cell orientation, either parallel or perpendicular to the underlying topographic features is also dependant on the constituents present in the soluble culture environment. In this study we also investigated the influence of sub-acuity topographic features on corneal cell contact guidance to larger topography. We fabricated substrates with 70 nm pitch WOS patterns overlaid in parallel to 4000 nm pitch (2000 nm groove) topographic features. We did not observe preferred cell orientation on 70 nm WOS alone. However, we observed a significant increase in the percentage of aligned cells on 4000 nm pitch with 70 nm WOS overlay compared to 4000 nm

pitch without the overlay. This result indicates that topographic features with sub-acuity dimensional values can still have an affect on cell contact guidance even though it does not elicit contact guidance on its own. These results will aid in the design of an improved synthetic corneal prosthetic because they highlight the influence of basement membrane dimensions on the contact guidance of human corneal epithelial cells.

Acknowledgments

The authors would like to thank Anna Kiyanova, Chi-Chun Liu and Yuk-Hong Ting for their excellent technical support. The authors would also like to thank Paul Russell, Teresa Porri and Greg King for their helpful discussions. Shared facilities of the Wisconsin Center for Applied Microelectronics and the Synchrotron Radiation Center at UW Madison were utilized to create silicon masters. This work is supported in part by 3M, NIH-National Eye Institute (1RO1EY017367-01A and 1RO1EY016134-01A2) and its contents are solely the responsibility of the authors and do not necessarily represent the official views of 3M, National Eye Institute or the NIH.

References

1. LeBleu VS, MacDonald B, Kalluri R. Structure and Function of Basement Membranes. Exp Biol Med 2007;232:1121–9.
2. Abe M, Osawa T. The structure of the interstitial surfaces of the epithelial basement membranes of mouse oral mucosa, gingiva and tongue. Arch Oral Biol 1999;44:587–94. [PubMed: 10414873]
3. Abrams GA, Bentley E, Nealey PF, Murphy CJ. Electron microscopy of the canine corneal basement membranes. Cells Tissues Organs 2002;170:251–7. [PubMed: 11919413]
4. Abrams GA, Goodman SL, Nealey PF, Franco M, Murphy CJ. Nanoscale topography of the basement membrane underlying the corneal epithelium of the rhesus macaque. Cell Tissue Res 2000;299:39–46. [PubMed: 10654068]
5. Abrams GA, Murphy CJ, Wang ZY, Nealey PF. Ultrastructural basement membrane topography of the bladder epithelium. Urol Res 2003;31:341–6. [PubMed: 14574540]
6. Abrams GA, Schaus SS, Goodman SL, Nealey PF, Murphy CJ. Nanoscale Topography of the Corneal Epithelial Basement Membrane and Descemet's Membrane of the Human. Cornea 2000;19:57–64. [PubMed: 10632010]
7. Brody S, Anilkumar T, Liliensiek S, Last JA, Murphy CJ, Pandit A. Characterizing Nanoscale Topography of the Aortic Heart Valve Basement Membrane for Tissue Engineering Heart Valve Scaffold Design. Tissue Eng 2006;12:413–21. [PubMed: 16548699]
8. Campbell S, Allen TD, Moser BB, Aplin JD. The translaminal fibrils of the human amnion basement membrane. J Cell Sci 1989;94:307–18. [PubMed: 2621227]
9. Howat WJ, Barabás T, Holmes JA, Holgate ST, Lackie PM. Distribution of basement membrane pores in bronchus revealed by microscopy following epithelial removal. J Struct Biol 2002;139:137–45. [PubMed: 12457843]
10. Last JA, Liliensiek SJ, Nealey PF, Murphy CJ. Determining the mechanical properties of human corneal basement membranes with atomic force microscopy. J Struct Biol 2009;167:19–24. [PubMed: 19341800]
11. Liliensiek SJ, Nealey P, Murphy CJ. Characterization of Endothelial Basement Membrane Nanotopography in Rhesus Macaque as a Guide for Vessel Tissue Engineering. Tissue Eng Part A 2009;15:2643–51. [PubMed: 19207042]
12. Osawa T, Nozaka Y. Scanning electron microscopic observation of the epidermal basement membrane with osmium conductive metal coating. J Electron Microsc (Tokyo) 1998;47:273–6. [PubMed: 9800377]
13. Shirato I, Tomino Y, Koide H, Sakai T. Fine structure of the glomerular basement membrane of the rat kidney visualized by high-resolution scanning electron microscopy. Cell Tissue Res 1991;266:1–10. [PubMed: 1747907]
14. Bush KA, Downing BR, Walsh SE, Pins GD. Conjugation of extracellular matrix proteins to basal lamina analogs enhances keratinocyte attachment. J Biomed Mater Res A 2007;80A:444–52. [PubMed: 17013864]

15. Alcaraz J, Xu R, Mori H, Nelson CM, Mroue R, Spencer VA, et al. Laminin and biomimetic extracellular elasticity enhance functional differentiation in mammary epithelia. EMBO J 2008;27:2829–38. [PubMed: 18843297]
16. Li ML, Aggeler J, Farson DA, Hatier C, Hassell J, Bissell MJ. Influence of a Reconstituted Basement Membrane and Its Components on Casein GeneExpression and Secretion in Mouse Mammary Epithelial Cells. Proc Natl Acad Sci U S A 1987;84:136–40. [PubMed: 3467345]
17. Chou SY, Cheng CM, LeDuc PR. Composite polymer systems with control of local substrate elasticity and their effect on cytoskeletal and morphological characteristics of adherent cells. Biomaterials 2009;30:3136–42. [PubMed: 19299009]
18. Lo CM, Wang HB, Dembo M, Wang YL. Cell movement is guided by the rigidity of the substrate. Biophys J 2000;79:144–52. [PubMed: 10866943]
19. Isenberg BC, DiMilla PA, Walker M, Kim S, Wong JY. Vascular Smooth Muscle Cell Durotaxis Depends on Substrate Stiffness Gradient Strength. Biophys J 2009;97:1313–22. [PubMed: 19720019]
20. Pelham RJ, Wang YL. Cell locomotion and focal adhesions are regulated by substrate flexibility. Proc Natl Acad Sci U S A 1997;94:13661–5. [PubMed: 9391082]
21. Banerjee A, Arha M, Choudhary S, Ashton RS, Bhatia SR, Schaffer DV, et al. The influence of hydrogel modulus on the proliferation and differentiation of encapsulated neural stem cells. Biomaterials 2009;30:4695–9. [PubMed: 19539367]
22. Engler AJ, Sen S, Sweeney HL, Discher DE. Matrix Elasticity Directs Stem Cell Lineage Specification. Cell 2006;126:677–89. [PubMed: 16923388]
23. Abrams, GA.; Teixeira, AI.; Nealey, PF.; Murphy, CJ. The effects of substratum topography on cell behavior. In: Dillow, AK.; Lowman, AM., editors. Biomimetic materials and design: biointerfacial strategies, tissue engineering, and targeted drug delivery. New York: Marcel Dekker; 2002. p. 91
24. Flemming RG, Murphy CJ, Abrams GA, Goodman SL, Nealey PF. Effects of synthetic micro- and nano-structured surfaces on cell behavior. Biomaterials 1999;20:573–88. [PubMed: 10213360]
25. Gasiorowski, JZ.; Foley, JD.; Russell, P.; Liliensiek, SJ.; Nealey, PF.; Murphy, CJ. Cellular Behavior on Basement Membrane Inspired Topographically Patterned Synthetic Matrices. In: Gonsalves, Kenneth E.; H, CR.; L, CT.; L, SN., editors. Biomedical Nanostructures. 2007. p. 297-319.
26. Teixeira AI, Abrams GA, Bertics PJ, Murphy CJ, Nealey PF. Epithelial contact guidance on well-defined micro- and nanostructured substrates. J Cell Sci 2003;116:1881–92. [PubMed: 12692189]
27. Teixeira AI, Abrams GA, Murphy CJ, Nealey PF. Cell behavior on lithographically defined nanostructured substrates. J Vac Sci Technol B 2003;21:683–7.
28. Teixeira AI, McKie GA, Foley JD, Bertics PJ, Nealey PF, Murphy CJ. The effect of environmental factors on the response of human corneal epithelial cells to nanoscale substrate topography. Biomaterials 2006;27:3945–54. [PubMed: 16580065]
29. Teixeira AI, Nealey PF, Murphy CJ. Responses of human keratocytes to micro- and nanostructured substrates. J Biomed Mater Res A 2004;71A:369–76. [PubMed: 15470741]
30. Liliensiek SJ, Campbell S, Nealey PF, Murphy CJ. The scale of substratum topographic features modulates proliferation of corneal epithelial cells and corneal fibroblasts. J Biomed Mater Res A 2006;79A:185–92. [PubMed: 16817223]
31. Karuri NW, Liliensiek S, Teixeira AI, Abrams G, Campbell S, Nealey PF, et al. Biological length scale topography enhances cell-substratum adhesion of human corneal epithelial cells. J Cell Sci 2004;117:3153–64. [PubMed: 15226393]
32. Karuri NW, Porri TJ, Albrecht RM, Murphy CJ, Nealey PF. Nano- and microscale holes modulate cell-substrate adhesion, cytoskeletal organization, and-beta 1 integrin localization in SV40 human corneal epithelial cells. IEEE Trans Nanobioscience 2006;5:273–80. [PubMed: 17181027]
33. Foley JD, Grunwald EW, Nealey PF, Murphy CJ. Cooperative modulation of neuritogenesis by PC12 cells by topography and nerve growth factor. Biomaterials 2005;26:3639–44. [PubMed: 15621254]
34. Yang F, Murugan R, Wang S, Ramakrishna S. Electrospinning of nano/micro scale poly(L-lactic acid) aligned fibers and their potential in neural tissue engineering. Biomaterials 2005;26:2603–10. [PubMed: 15585263]

35. Park J, Bauer S, Schmuki P, von der Mark K. Narrow Window in Nanoscale Dependent Activation of Endothelial Cell Growth and Differentiation on TiO2 Nanotube Surfaces. Nano Lett 2009;9:3157–64. [PubMed: 19653637]
36. Dalby MJ, Gadegaard N, Riehle MO, Wilkinson CDW, Curtis ASG. Investigating filopodia sensing using arrays of defined nano-pits down to 35 nm diameter in size. Int J Biochem Cell Biol 2004;36:2005–15. [PubMed: 15203114]
37. Loesberg WA, te Riet J, van Delft FCMJM, Schön P, Figdor CG, Speller S, et al. The threshold at which substrate nanogroove dimensions may influence fibroblast alignment and adhesion. Biomaterials 2007;28:3944–51. [PubMed: 17576010]
38. Fraser SA, Ting YH, Wendt AE, Murphy CJ, Nealey PF. Sub-micron and nanoscale feature depth modulates alignment of stromal fibroblasts and corneal epithelial cells in serum-rich and serum-free media. J Biomed Mater Res A 2008;86A:725–35. [PubMed: 18041718]
39. Smirnov VK, Kibalov DS, Krivelevich SA, Lepshin PA, Potapov EV, Yankov RA, et al. Wave-ordered structures formed on SOI wafers by reactive ion beams. Nucl Inst and Meth B 1999;147:310–5.
40. Smirnov VK, Kibalov DS, Orlov OM, Graboshnikov VV. Technology for nanoperiodic doping of a metal–oxide–semiconductor field-effect transistor channel using a self-forming wave-ordered structure. Nanotechnology 2003;14:709–15.
41. Allen-Hoffmann BL, Rheinwald JG. Polycyclic aromatic hydrocarbon mutagenesis of human epidermal keratinocytes in culture. Proc Natl Acad Sci U S A 1984;81:7802–6. [PubMed: 6440145]
42. Sabatini LM, Allen-Hoffmann BL, Warner TF, Azen EA. Serial Cultivation of Epithelial Cells from Human and Macaque Salivary Glands. In Vitro Cell Dev Biol 1991;27A:939–48. [PubMed: 1721908]
43. Gerecht S, Bettinger CJ, Zhang Z, Borenstein JT, Vunjak-Novakovic G, Langer R. The effect of actin disrupting agents on contact guidance of human embryonic stem cells. Biomaterials 2007;28:4068–77. [PubMed: 17576011]
44. Rajnicek A, McCaig C. Guidance of CNS growth cones by substratum grooves and ridges: effects of inhibitors of the cytoskeleton, calcium channels and signal transduction pathways. J Cell Sci 1997;110:2915–24. [PubMed: 9359874]
45. Rajnicek AM, Foubister LE, McCaig CD. Alignment of corneal and lens epithelial cells by co-operative effects of substratum topography and DC electric fields. Biomaterials 2008;29:2082–95. [PubMed: 18281089]
46. Vrana E, Builles N, Hindie M, Damour O, Aydinli A, Hasirci V. Contact guidance enhances the quality of a tissue engineered corneal stroma. J Biomed Mater Res A 2008;84A:454–63. [PubMed: 17618494]
47. Manwaring ME, Walsh JF, Tresco PA. Contact guidance induced organization of extracellular matrix. Biomaterials 2004;25:3631–8. [PubMed: 15020137]
48. Biela SA, Su Y, Spatz JP, Kemkemer R. Different sensitivity of human endothelial cells, smooth muscle cells and fibroblasts to topography in the nano-micro range. Acta Biomater 2009;5:2460–6. [PubMed: 19410529]
49. Schumacher JF, Aldred N, Callow ME, Finlay JA, Callow JA, Clare AS, et al. Species-specific engineered antifouling topographies: correlations between the settlement of algal zoospores and barnacle cyprids. Biofouling 2007;23:307–17. [PubMed: 17852066]

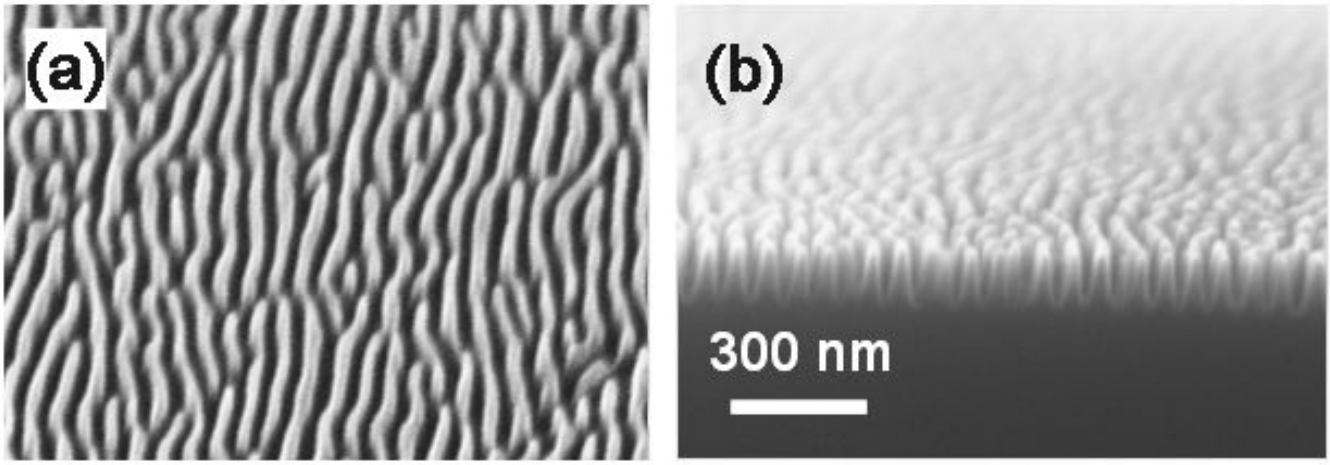

Figure 1.
SEM of 90 nm WOS substrates (a) top down and (b) cross section.

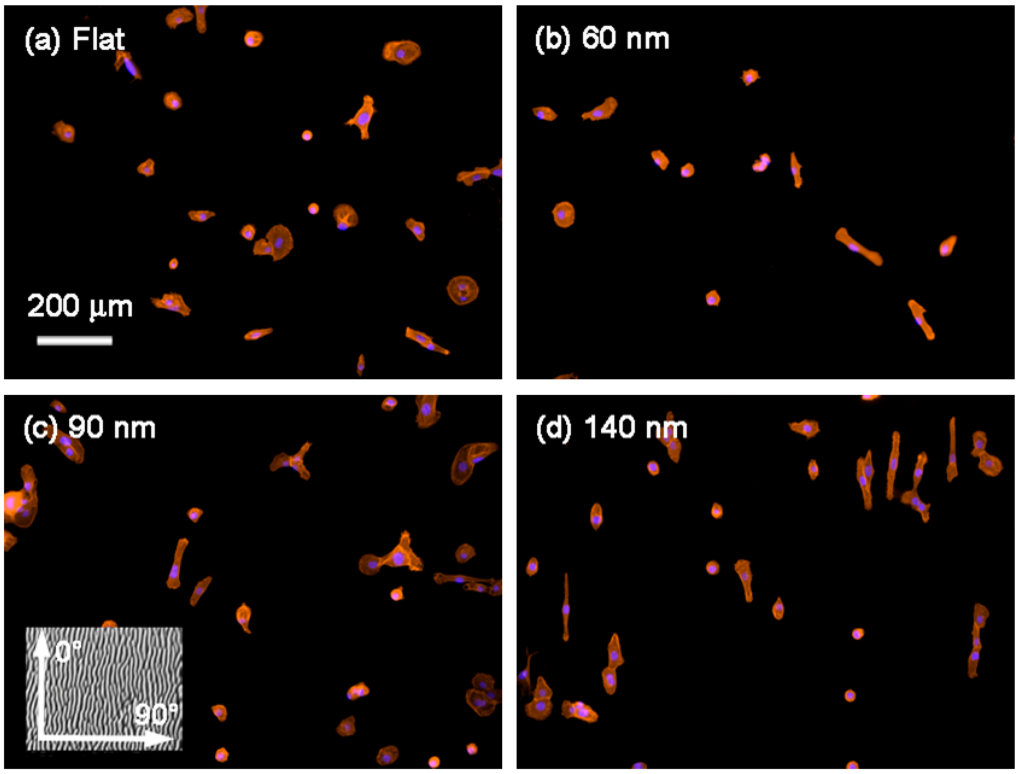

Figure 2.
In epithelial medium, we observed an increase in parallel alignment to WOS topography (oriented as shown in inset of (c)) with pitches 90 nm (c), and 140 nm (d) compared to flat controls (a) and 60 nm WOS (b). Cells were fixed 12 hours post plating and stained with actin-phalloidin (red) and nuclear stain DAPI (blue).

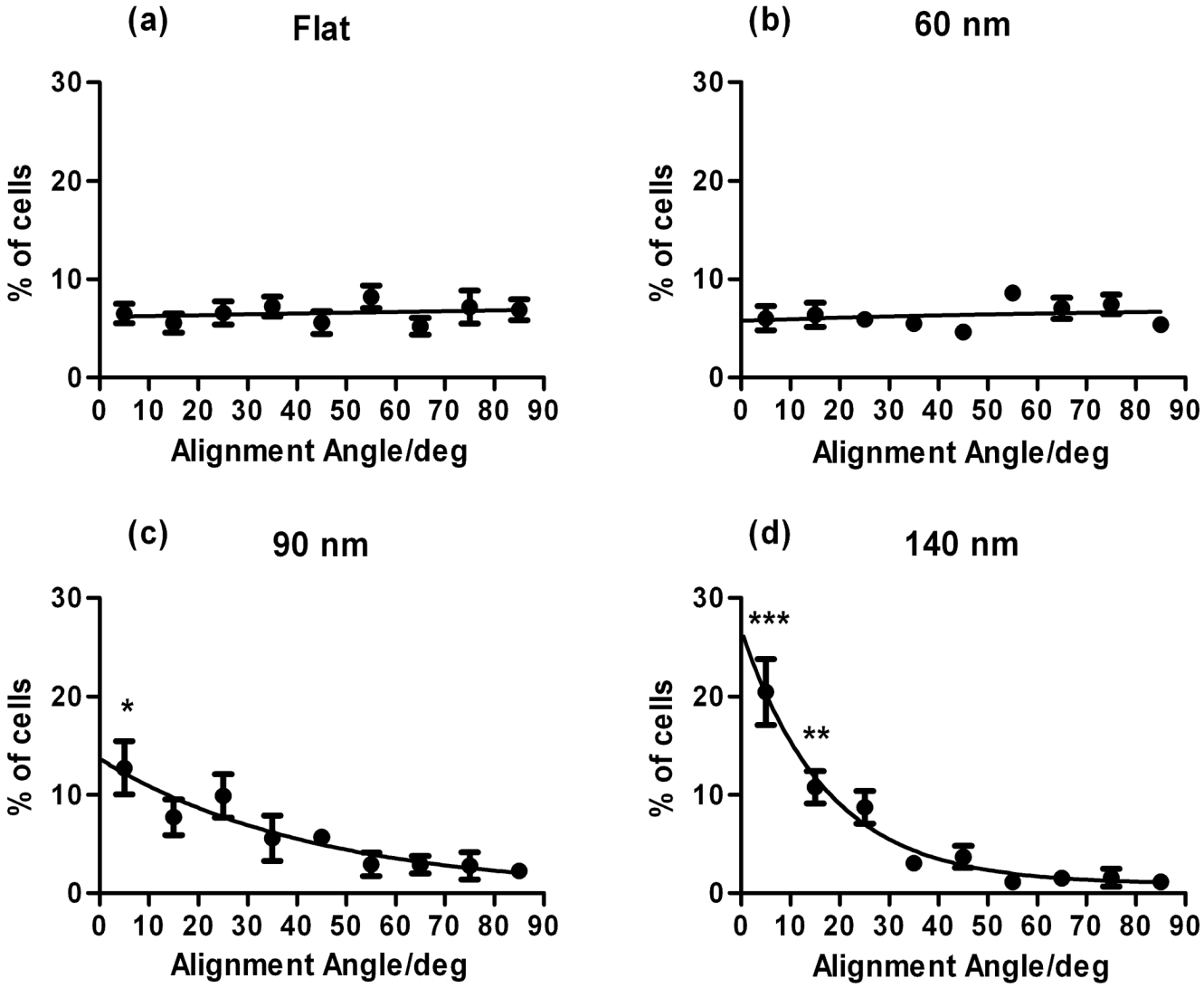

Figure 3.

In epithelial medium, HCEC did not have a preferred angle of alignment to flat controls (a) nor 60 nm WOS substrates (b). On 90 nm (c) and 140 nm (d) WOS, there was a significant trend for cells to align parallel (0-10 degrees) to the topography. (* $0.01<P<0.05$, ** $0.001<P<0.01$, *** $P<0.001$ compared to other angles within each graph)

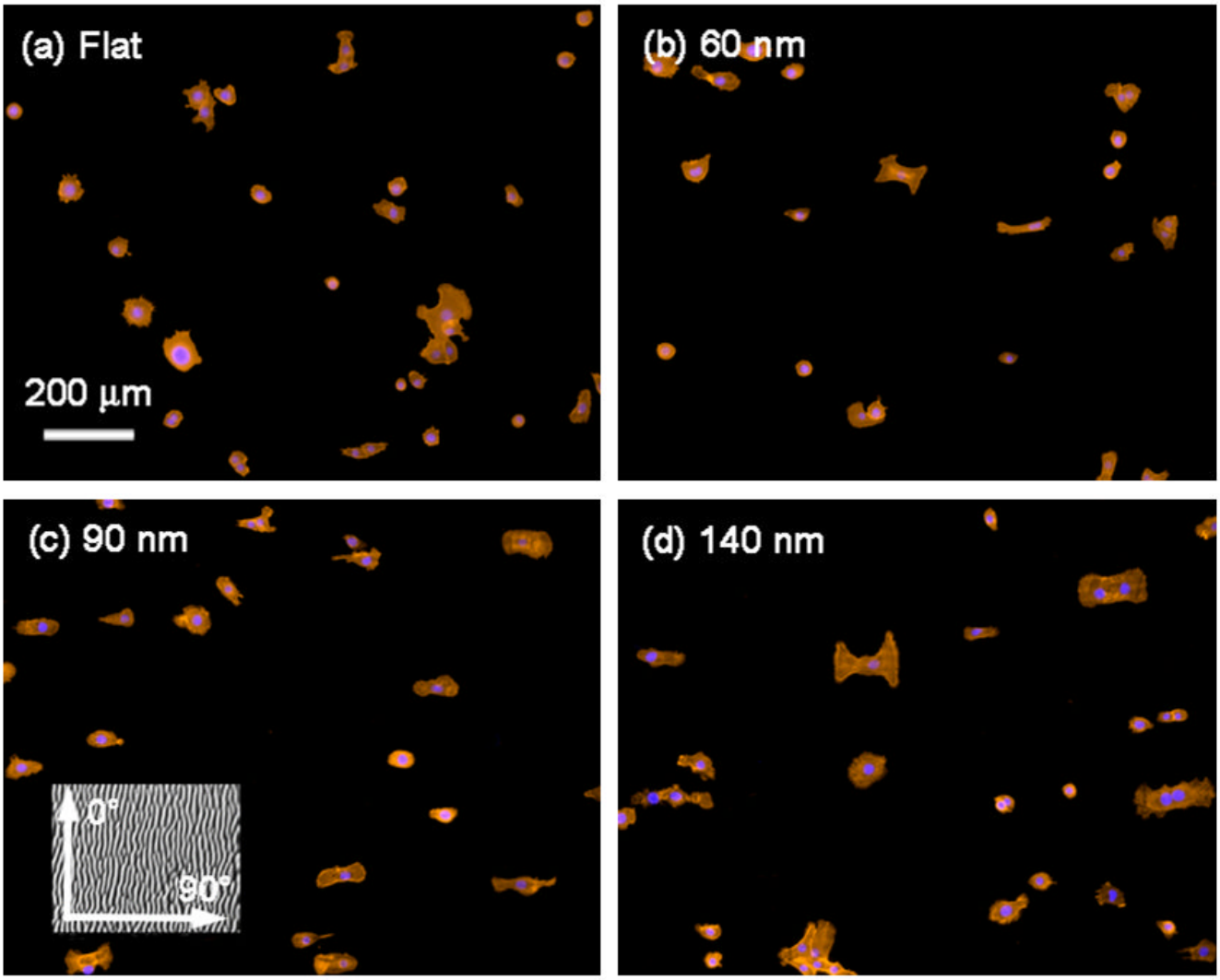

Figure 4.
In EpiLife® medium, we observed an increase in HCEC perpendicular alignment to WOS topography (oriented as shown in inset of (c)) with pitches 60 nm (b), 90 nm (c), and 140 nm (d) compared to flat controls (a). Cells were fixed 12 hours post plating and stained with actin-phalloidin (red) and nuclear stain DAPI (blue).

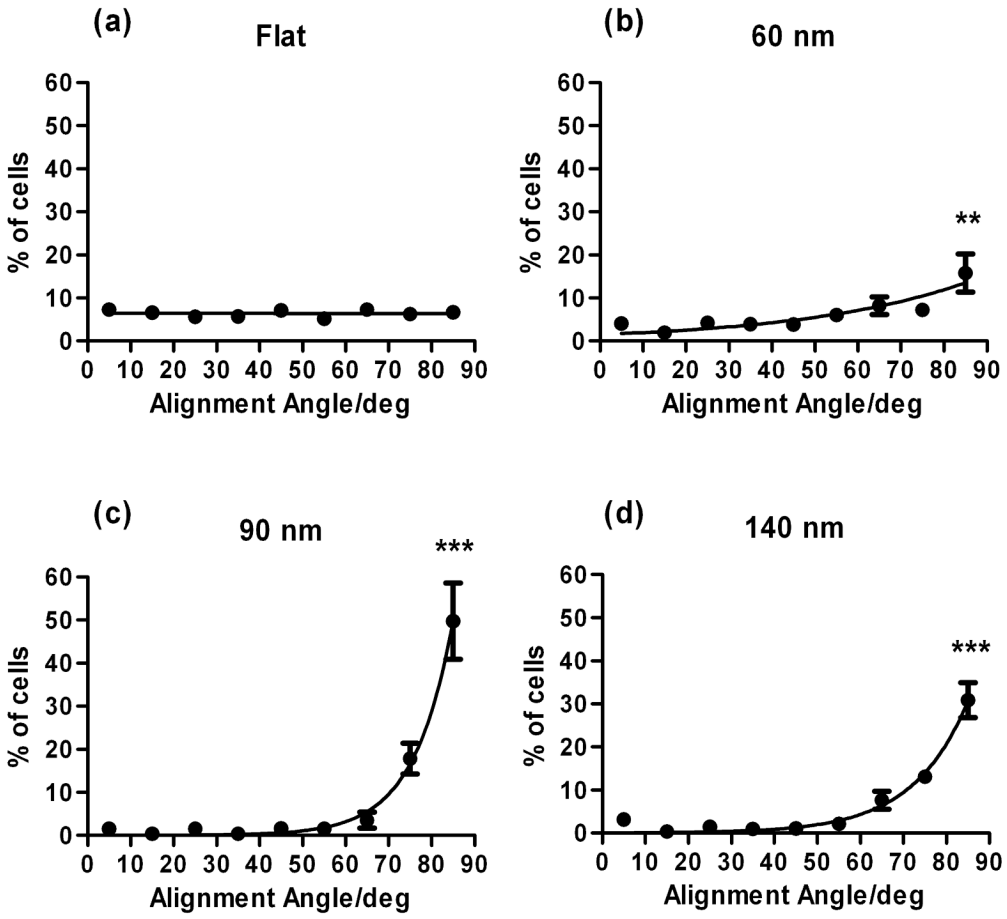

Figure 5.

In EpiLife® medium, HCEC did not have a preferred angle of alignment to flat controls. However, on (a) 60 nm, (b) 90 nm (c) and 140 nm (d) WOS, there were significant trends showing that the cells aligned perpendicular (80-90 degrees) to the topography. (* $0.01<P<0.05$, ** $0.001<P<0.01$, *** $P<0.001$ compared to other angles within each graph)

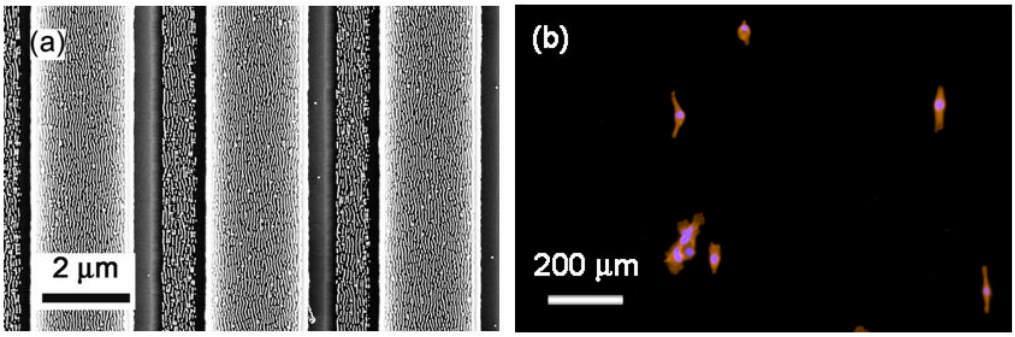

Figure 6.
(a) SEM of 70 nm WOS overlaid on 4000 nm pitch (400 nm deep) ridge and groove structures. (b) Fluorescent image of HCEC in epithelial medium show parallel alignment to substrate as depicted in (a).

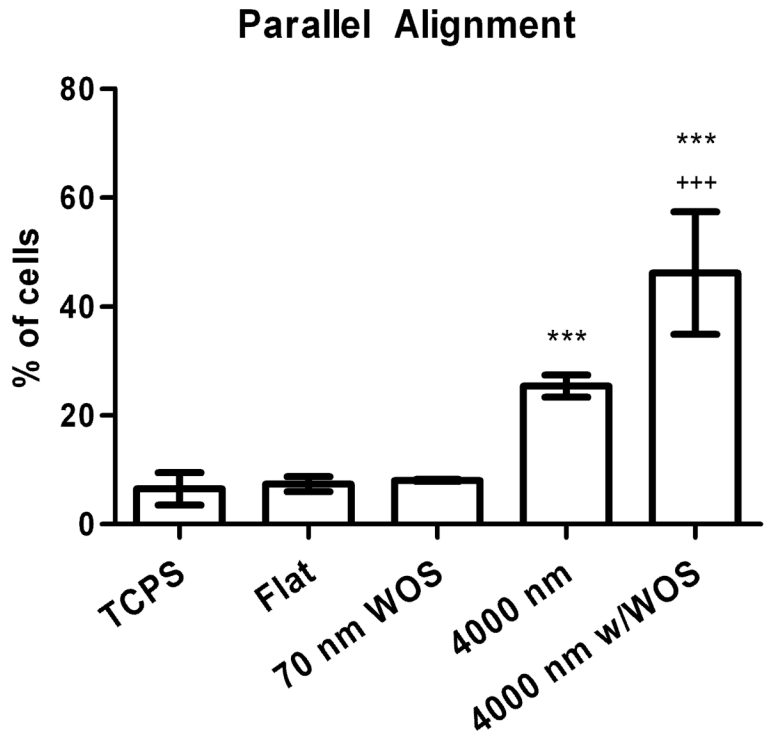

Figure 7.

HCEC in epithelial medium showed significant increase in parallel alignment to 4000 nm ridge-groove features compared to TCPS, flat and 70 nm WOS controls. Additionally, HCEC showed significant increase in parallel alignment on 4000 nm ridge-groove features with 70 nm WOS overlay compared to controls and 4000 nm ridge-groove features. (*** $P<0.001$ compared to TCPS, Flat, and 70 nm WOS; +++ $P<0.001$ compared to 4000 nm ridge-groove features)